Benzodiazepine Receptors in Chronic Cerebrovascular Disease: Comparison with Blood Flow and Metabolism

Masayuki Sasaki, Yuichi Ichiya, Yasuo Kuwabara, Tsuyoshi Yoshida, Toshimitsu Fukumura and Kouji Masuda
Department of Radiology, Faculty of Medicine, Kyushu University, Fukuoka, Japan

The brain benzodiazepine (BZD) receptor distribution in patients with chronic cerebrovascular disease was assessed with ^{123}I-iomazenil (IMZ) SPECT, and the findings were compared with the data for the cerebral blood flow (CBF) and cerebral metabolism. **Methods:** We examined nine patients with chronic cerebrovascular diseases, six patients with cerebral infarction and three with moyamoya disease. Iodine-123-IMZ SPECT images were obtained for 15 min, 3 hr after the administration of 167 or 222 MBq ^{123}I-IMZ. In seven patients, the CBF and oxygen metabolism were measured by the ^{15}O steady-state method. In two patients, the CBF and glucose metabolism were measured by ^{99m}Tc-HMPAO SPECT and ^{18}F-fluoro-2-deoxy-D-glucose-PET, respectively. The brain was initially classified into 18 regions, and abnormalities in the BZD receptor distribution, CBF and cerebral metabolism were visually evaluated. The count ratio of lesion-to-contralateral normal region (L-to-C ratio) was then used for comparison. **Results:** In the core of the infarct, the ^{123}I-IMZ uptake decreased (L-to-C ratios of the blood flow 0.42 ± 0.26; metabolism 0.45 ± 0.24; and ^{123}I-IMZ uptake 0.46 ± 0.14). In the peri-infarct region, the ^{123}I-IMZ uptake slightly decreased (L-to-C ratios of 0.81, 0.82 and 0.89, respectively). In the region of misery perfusion, the ^{123}I-IMZ uptake was preserved (L-to-C ratios of 0.73, 1.07 and 1.02, respectively). In the remote deafferentated areas in the ipsilateral cerebrum, the ^{123}I-IMZ uptake was preserved (L-to-C ratios of 0.76 ± 0.10, 0.75 ± 0.04 and 0.98 ± 0.05, respectively). In the remote areas in the contralateral cerebellum, the ^{123}I-IMZ uptake was preserved (L-to-C ratios of 0.84 ± 0.08, 0.85 ± 0.04 and 0.94 ± 0.05, respectively). **Conclusion:** The BZD receptor distribution, as measured by ^{123}I-IMZ SPECT, is not considered to reflect neuronal function, but it may reflect neuronal cell viability. Iodine-123-IMZ SPECT may, therefore, hold promise as a potential probe for neuronal damage.

Key Words: Iodine-123-iomazenil; benzodiazepine receptor; SPECT; PET

J Nucl Med 1997; 38:1693–1698

In patients with cerebrovascular disease, the measurement of both the cerebral blood flow (CBF) and cerebral metabolism is useful for the evaluation of ischemic changes in the brain. Although the CBF is evaluated by either SPECT or PET, whereas the cerebral metabolism is evaluated by PET, neuronal damage can be assessed only by morphological diagnosis using either magnetic resonance imaging (MRI) or x-irradiation CT. In some patients with cerebrovascular disease, discrepancies between the blood flow, metabolism and morphological changes are observed. However, neuronal damage, especially with minimal morphological changes, cannot be evaluated by any of these imaging modalities.

Central benzodiazepine (BZD) receptors are thought to exist in the membrane of neurons and to be coupled with gamma-amino butyric acid receptors. Central BZD receptors are thus considered to play an important inhibitory function in the brain. In vivo measurement of the central BZD receptor density has been performed using ^{11}C-flumazenil and PET (*1–4*). Clinically, ^{11}C-flumazenil PET has been reported to be useful for the detection of epileptic foci (*5,6*). Iodine-123-RO 16-0154 (ethyl-5,6-dihydro-7-iodo-5-methyl-6-oxo-4H-imidazo[1,5-a][1,4]-benzodiazepine-3-carboxylate), also known as iomazenil (IMZ), is a high-affinity radioligand used for the assessment of central BZD receptors with SPECT (*7*). Its usefulness has been reported in the diagnosis of both focal epilepsy (*8,9*) and Alzheimer's disease (*10*).

Sette et al. (*11*) examined the effect of ischemic changes on BZD receptors in baboons with unilateral middle cerebral artery occlusion and observed decreased ^{11}C-flumazenil uptake in the infarcted areas and preservation of ^{11}C-flumazenil uptake in the deafferentated hypometabolic cortical areas. Recently, Hatazawa et al. (*12*) evaluated changes in the central BZD receptors in patients with cerebral infarction using ^{123}I-IMZ SPECT and observed decreased ^{123}I-IMZ uptake in the infarcted areas and preservation of ^{123}I-IMZ uptake in the deafferentated cortical areas. Central BZD receptors are thus thought to be a potential marker for neuronal damage.

In this study, we assessed the central BZD receptor distribution in patients with chronic cerebrovascular diseases using ^{123}I-IMZ SPECT and compared the findings with those for the CBF and cerebral metabolism. The purpose of this study was to assess the usefulness of the BZD receptor distribution as a potential probe for evaluating neuronal damage.

MATERIALS AND METHODS

Patients

We examined nine patients with chronic cerebrovascular disease, six with cerebral infarction and three with moyamoya disease (five men, four women; aged 34–67 yr; mean age 52 ± 12 yr). All examinations were performed at least 2 mo after the last ischemic attack. The patient characteristics are summarized in Table 1. In seven patients, the CBF and oxygen metabolism were measured by the ^{15}O steady-state method. In two patients, the CBF and glucose metabolism were measured by ^{99m}Tc-HMPAO SPECT and ^{18}F-fluoro-2-deoxy-D-glucose (FDG)-PET, respectively. No BZD receptor agonists were administered to any of the patients from at least 2 mo before the initiation of the study. This study was approved by the Committee for Clinical Application of Cyclotron-produced Radionuclides in Kyushu University Hospital. Written informed consent was received from all patients before study initiation.

Iodine-123-Iomazenil SPECT Protocol

To evaluate the BZD receptor distribution, data acquisition was performed for 15 min, beginning 172 min after the administration of 167 or 222 MBq ^{123}I-IMZ, using a three-detector system GCA9300A/HG (Toshiba Corp., Tokyo, Japan) with a fanbeam collimator (64 × 64 matrix). Each detector was set to rotate continuously through 120° in 3 min, alternating in the clockwise and counterclockwise directions. A Butterworth filter, with a cutoff

Received Jul. 18. 1996; revision accepted Mar. 4, 1997.
For correspondence or reprints contact: Masayuki Sasaki, MD, PhD, Department of Radiology, Faculty of Medicine, Kyushu University, 3-1-1 Maidashi, Higashi-ku, Fukuoka 812-82, Japan.

TABLE 1
Patient Characteristics

Patient no.	Age (yr)	Sex	Clinical diagnosis	Infarction			Examinations	
				Location	Size (cm)	Time after onset	CBF	Metabolism
1	56	M	Cerebral infarction	R frontal cortex	2.5 × 2.0	3 mo	$H_2{}^{15}O$	$^{15}O_2$
2	64	F	Cerebral infarction	L basal ganglia	1.5 × 1.0	2 mo	$H_2{}^{15}O$	$^{15}O_2$
3	67	M	Cerebral infarction	L basal ganglia	<0.5	2 yr	$H_2{}^{15}O$	$^{15}O_2$
4	48	M	Cerebral infarction	R pons	<0.5	5 mo	$H_2{}^{15}O$	$^{15}O_2$
5	63	F	Cerebral infarction	R thalamus	1.5 × 1.0	7 yr	^{99m}Tc-HMPAO	^{18}F-FDG
6	56	M	Cerebral infarction	R basal ganglia	0.5 × 0.5	5 yr	^{99m}Tc-HMPAO	^{18}F-FDG
7	34	M	Moyamoya disease	R frontal cortex,	2.0 × 2.0	1 yr	$H_2{}^{15}O$	$^{15}O_2$
				L temporal white matter	4.0 × 4.0	6 yr		
8	44	F	Moyamoya disease	R temporal cortex	3.5 × 2.0	1 yr	$H_2{}^{15}O$	$^{15}O_2$
9	35	F	Moyamoya disease	R temporal cortex,	2.5 × 2.0	6 mo	$H_2{}^{15}O$	$^{15}O_2$
				L frontal cortex	2.0 × 2.0	1 yr		

R = right; L = left.

of 0.24 cycle/cm and an order of 8, and a ramp filter were used for image reconstruction. Attenuation correction was performed using an attenuation coefficient of 0.12 cm^{-1}. The spatial resolution in plane was 7.4 mm of FWHM.

Measurement of Cerebral Blood Flow

The CBF was measured by the ^{15}O steady-state method in seven patients and by ^{99m}Tc-HMPAO SPECT in two patients.

The regional CBF (rCBF; ml/min/100 ml) was measured by the ^{15}O steady-state method as described previously (*13,14*). After transmission scanning with a $^{68}Ge/^{68}Ga$ ring source for attenuation correction, $H_2{}^{15}O$ was continuously infused through a medial cubital vein. Upon reaching equilibrium, data were acquired for 6 min with a HEADTOME III (Shimadzu Corp. and Akita Noken, Kyoto, Japan). Five slices, each 15 mm apart, were obtained. The spatial resolution in plane was 8.2 mm of FWHM.

To obtain ^{99m}Tc-HMPAO SPECT images, data acquisition were performed for 15 min, beginning 5 min after administration of 740 MBq ^{99m}Tc-HMPAO, using the SPECT device described above. The ^{99m}Tc-HMPAO SPECT images were corrected by Lassen et al.'s method (*15*). The cerebellar hemisphere without remote effect was used as the reference region. Quantification of the absolute rCBF value was not performed in ^{99m}Tc-HMPAO SPECT.

Measurement of Cerebral Metabolism

The oxygen metabolism was measured by the ^{15}O steady-state method in seven patients, and glucose metabolism was measured by FDG method in two patients, respectively, using the same PET device as described above.

For measuring the regional cerebral metabolic rate for oxygen ($rCMRO_2$; ml/min/100 ml), $^{15}O_2$ was continuously inhaled (*13,14*). After equilibrium was reached, data were acquired for 7 min. The regional cerebral blood volume (ml/100 ml) was measured by inhalation of $C^{15}O$ in a single bolus breath, and the value obtained was used for the correction of $rCMRO_2$ and the regional oxygen extraction fraction (rOEF; %) (*16*).

The regional cerebral metabolic rate for glucose (rCMRGlc; mg/min/100 ml) was determined from the 8-min scan commencing from 63 min after administration of 185 MBq of FDG. The model of Phelps et al. (*17*), later modified by Brooks (*18*), was used with a lumped constant of 0.42.

Data Analysis

For visual analysis of SPECT and PET images, the brain was classified into 18 regions according to the anatomical classification shown in Figure 1. Abnormalities in the CBF, cerebral metabolism and BZD receptor distribution were visually evaluated by three nuclear medicine physicians.

Rectangular regions of interest (ROIs), 18 × 14 mm on PET images and 17 × 14 mm on SPECT images, were carefully placed on the basis of visual comparison of images to select the same lesion, because coregistration of the MRI, SPECT images and PET images was not performed in this analysis. Only one ROI was placed in each lesion to estimate the value of the lesion in each patient. Reference ROIs were placed in the contralateral, apparently normal region with normal perfusion, normal metabolism and no morphological abnormalities. The count ratio of the lesion-to-contralateral normal region was defined as the L-to-C ratio. In cases with moyamoya disease (Patients 7 and 9), multiple lesions were observed in the bilateral cerebral cortices. In these cases, the reference regions were not exactly the contralateral mirror region but were placed in an apparently normal area with normal perfusion and normal metabolism near the mirror region in the contralateral cerebral artery territory. Statistical significance was determined by the paired Student's t-test.

Assessment of the Pathophysiological Status of Lesions

The pathophysiological status of lesions was determined from both the blood flow and the metabolism in addition to morphological diagnosis of MR images. A 1.5-T superconducting unit was used for MR imaging. T1-weighted spin-echo images were obtained with a sequence of 500/18/1 (TR/TE/excitations). T2-weighted fast spin-echo images were obtained with a sequence of

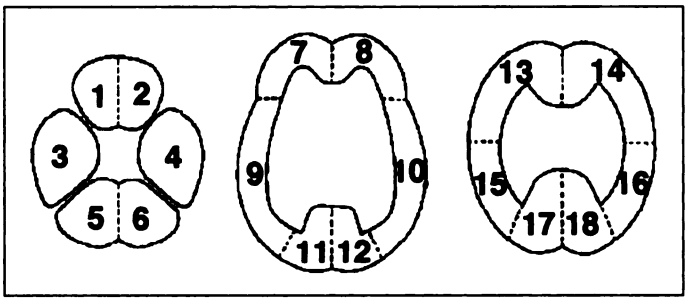

FIGURE 1. The diagrams show the definition of regions for visual comparison of SPECT and PET images: 1 and 2, right and left inferior frontal regions, respectively; 3 and 4, right and left inferior temporal regions, respectively; 5 and 6, right and left cerebellar hemispheres, respectively; 7 and 8, right and left middle frontal regions, respectively; 9 and 10, right and left middle temporal regions, respectively; 11 and 12, right and left inferior occipital regions, respectively; 13 and 14, right and left superior frontal regions, respectively; 15 and 16, right and left parietal regions, respectively; 17 and 18, right and left superior occipital regions, respectively.

TABLE 2
Comparison of the Numbers of Abnormal Regions

CBF	Metabolism	^{123}I-IMZ uptake (no. of regions) Normal	Decreased
Normal	Normal	113	0
	Decreased	0	0
Decreased	Normal	9	0
	Decreased	31	9

2500/110/1. The imaging parameters were 256 × 192 matrix, 23 × 17-cm field of view and 5-mm slice thickness with a 2.5-mm slice gap.

The infarct area was defined as an area with T1- and T2-prolongation on MRI. The peri-infarct area was defined as an area with normal MRI findings with both hypoperfusion and hypometabolism surrounding the infarct area. Misery perfusion was defined as an area with normal MRI findings and an OEF of 15% or higher than that of the contralateral region. The remote area in the cerebrum was defined as an area with normal MRI findings and both hypoperfusion and hypometabolism in the ipsilateral cerebral cortex due to infarction in the subcortical region. The remote area in the cerebellum was defined as an area with normal MRI findings and both hypoperfusion and hypometabolism in the contralateral cerebellum due to infarction in the cerebro-cerebellar neuronal pathway. Only one ROI was placed in each lesion to represent the value of the lesion in each patient, even if there were either multiple lesions or broad extensive lesions covering several regions. Lesions smaller than 2 cm in diameter were eliminated from this measurement because of the limitation in spatial resolution of our devices.

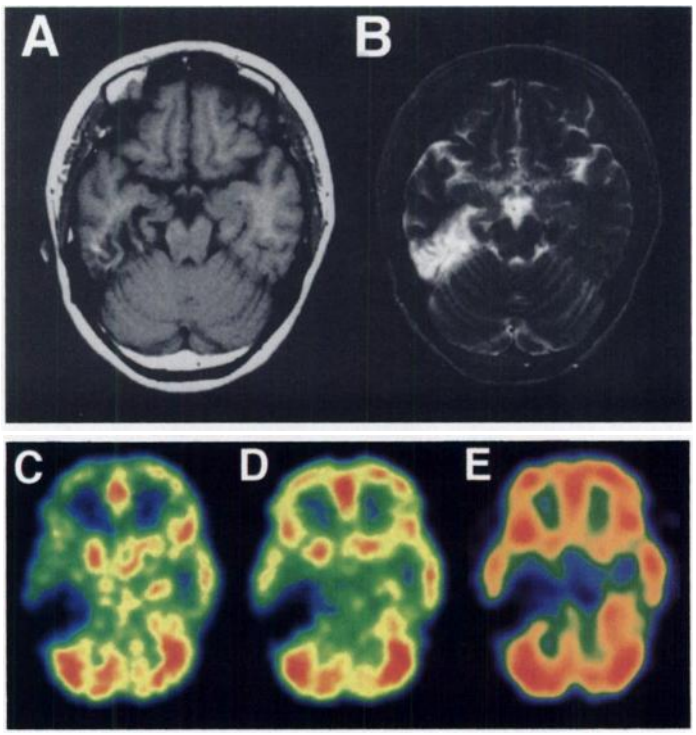

FIGURE 2. Patient 8, a 44-yr-old woman with moyamoya disease. (A) T1-weighted MR image; (B) T2-weighted MR image; (C) CBF-PET; (D) $CMRO_2$; (E) ^{123}I-IMZ SPECT, all obtained 35 mm above and parallel to the OM line. The posterior part of the right temporal lobe shows an infarcted area with T1- and T2-prolongation. A perfusion defect, reduced $CMRO_2$ and reduced uptake of ^{123}I-IMZ are observed in the lesion. The right frontal lobe is diagnosed as a lesion with misery perfusion because of the decreased CBF and preserved $CMRO_2$ without any abnormalities on the MR images. Iodine-123-IMZ uptake was preserved in the lesion with misery perfusion.

RESULTS

Comparison of Abnormalities in Blood Flow, Metabolism and Benzodiazepine Receptors

Abnormalities of the blood flow, metabolism and ^{123}I-IMZ uptake were visually evaluated, and the numbers of abnormal regions in each image were compared (Table 2). In 113 of the total 162 regions, the CBF, cerebral metabolism and ^{123}I-IMZ uptake were all preserved. In 49 of the 162 regions, a decrease in the CBF was observed. In nine regions with hypoperfusion and hypometabolism, ^{123}I-IMZ uptake showed a decrease. These regions proved to be the core of the infarct in seven regions or the peri-infarcted area in two regions. In nine regions with hypoperfusion and preserved cerebral metabolism (misery perfusion), ^{123}I-IMZ uptake was preserved (Fig. 2; Patient 8). In spite of hypoperfusion and hypometabolism, in 31 regions, ^{123}I-IMZ uptake was preserved. These regions proved to be remote deafferentated areas, including 26 regions in the ipsilateral cerebral cortices (Fig. 3; Patient 2) and five in the contralateral cerebellum (so-called crossed cerebellar diaschisis). There were no regions with luxury perfusion in any of the patients in this study. The absolute values for the CBF, OEF and cerebral metabolism in lesions are summarized in Table 3.

Lesion-to-Contralateral Normal Region Ratios for Blood Flow, Metabolism and Benzodiazepine Receptors

The mean L-to-C ratios of the blood flow, metabolism and ^{123}I-IMZ uptake are shown in Figure 4. The mean L-to-C ratios of the infarcts (n = 4) were 0.42 ± 0.26 for the blood flow, 0.45 ± 0.24 for the metabolism and 0.46 ± 0.14 for the ^{123}I-IMZ uptake. In the peri-infarct area (n = 1), the ratios were 0.81 for the blood flow, 0.82 for the metabolism and 0.89 for the ^{123}I-IMZ uptake. In the misery perfused areas (n = 2), the ratios were 0.73 for the blood flow, 1.07 for the metabolism and 1.02 for the ^{123}I-IMZ uptake. In the remote areas of the cerebrum (n = 4), the ratios were 0.76 ± 0.10 for the blood flow, 0.75 ± 0.04 for the metabolism and 0.98 ± 0.05 for the ^{123}I-IMZ uptake. Both the blood flow and metabolism showed a significant decrease compared to the ^{123}I-IMZ uptake ($p < 0.05$ and $p < 0.01$, respectively). In the remote areas of the cerebellum (n = 5), the ratios were 0.84 ± 0.08 for the blood flow, 0.85 ± 0.04 for the metabolism and 0.94 ± 0.05 for the ^{123}I-IMZ uptake. The metabolism showed a significant decrease compared to the ^{123}I-IMZ uptake ($p < 0.05$).

DISCUSSION

Benzodiazepine Receptors

The changes in BZD receptors in chronic cerebral infarction have been studied in animal models using autoradiographic techniques. Onodera et al. (*19*) observed a decrease in ^{3}H-flunitrazepam uptake in ischemic necrosis of the rat brain 27 days after transient ischemia. Recently, there have been reports of a decrease in either ^{125}I- or ^{123}I-IMZ uptake in chronic cerebral infarction after permanent occlusion of a unilateral middle cerebral artery (*20,21*). In vivo mapping of BZD receptors was performed by Sette et al. (*11*) using ^{11}C-flumazenil and PET in anesthetized baboons after unilateral middle cerebral artery occlusion. They observed a significant decrease in ^{11}C-flumazenil uptake in the infarcted area from day 2 to day 54, suggesting a decrease in the BZD receptor density. Using SPECT in patients with cerebral infarction, ^{123}I-IMZ uptake in the infarct showed a significant decrease (*12*). There was no significant time-dependent change in ^{123}I-IMZ uptake from day 4 to day 196. In this study, a decrease in ^{123}I-IMZ

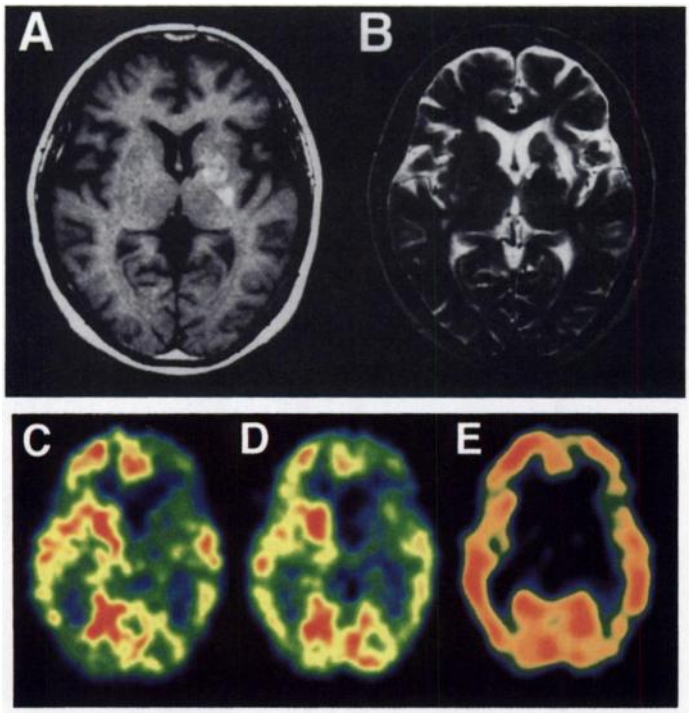

FIGURE 3. Patient 2, a 64-yr-old woman with cerebral infarction in the left basal ganglia. (A) T1-weighted MR image; (B) T2-weighted MR image; (C) CBF-PET; (D) $CMRO_2$; (E) ^{123}I-IMZ SPECT, all obtained 50 mm above and parallel to the OM line. MR images demonstrate an infarct in the left basal ganglia and left internal capsule. A perfusion defect, reduced $CMRO_2$ and reduced uptake of ^{123}I-IMZ are observed in the lesion. The left frontal lobe is diagnosed as a remote deafferentated area because of a decreased CBF and decreased $CMRO_2$ with minimal cortical atrophy on MR images. The change in ^{123}I-IMZ uptake was minimal in the remote deafferentated area.

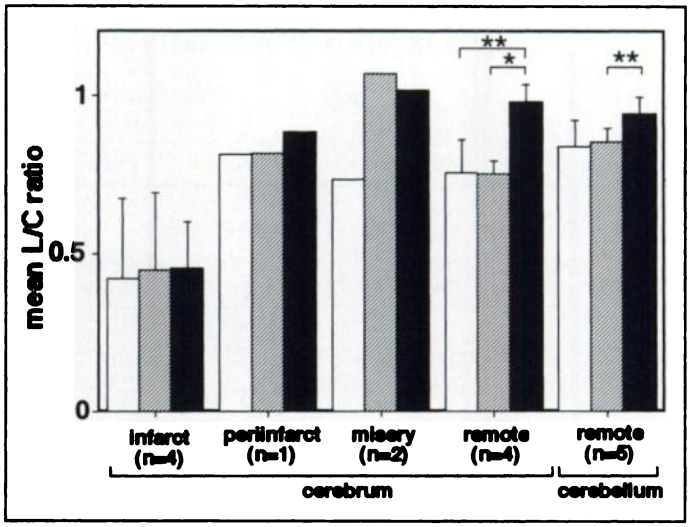

FIGURE 4. Mean L-to-C ratios of blood flow, metabolism and ^{123}I-IMZ uptake in lesions. □, CBF; ▨, cerebral metabolism; ■, ^{123}I-IMZ uptake. Statistical significance was determined by paired Student's t-test: *, $p < 0.01$; **, $p < 0.05$.

uptake was observed in seven regions with chronic infarction from 2 mo to 7 yr after onset. This result is consistent with those of previous studies and suggests that ^{123}I-IMZ uptake reflects the BZD receptor distribution and, hence, neuronal cell viability.

The decrease in BZD receptor density in chronic cerebral infarction has been reported to be more prominent than the decrease in either the blood flow examined by ^{99m}Tc-HMPAO (*20*) or the ^{14}C-2-deoxyglucose uptake (*21*). Such differences are thought to be caused by residual blood flow and metabolism of gliotic reactions and by the infiltration of macrophages. In this study, the degree of decrease in ^{123}I-IMZ uptake did not differ from the decrease in either the blood flow or metabolism. This result may suggest that either complete destruction of neurons did not occur or BZD receptors were still present in spite of the neuronal damage in the infarct area.

Benzodiazepine Receptors in the Peri-Infarct Area

In this study, a decrease in ^{123}I-IMZ uptake was observed in the peri-infarct area, and it was associated with both a decrease in blood flow and a decrease in metabolism in the same area. Hypoperfusion and hypometabolism without morphological changes on MR images may suggest either minimal neuronal damage or deafferentation in the peri-infarct area. Neuronal loss in the area surrounding chronic infarction has been observed in

TABLE 3
Cerebral Blood Flow, Oxygen Extraction Fraction, Cerebral Metabolic Rate for Oxygen and Cerebral Metabolic Rate for Glucose in Lesions and the Contralateral Region

		Affected region				Contralateral region			
Lesion	Patient no.	rCBF (ml/min/100ml)	rOEF (%)	$rCMRO_2$ (ml/min/100ml)	rCMRGlc (mg/min/100ml)	rCBF (ml/min/100ml)	rOEF (%)	$rCMRO_2$ (ml/min/100ml)	rCMRGlc (mg/min/100ml)
Infarct	1	22.0	33.7	1.51	—	29.3	36.8	2.19	—
	7	5.2	44.2	0.29	—	38.3	42.8	2.44	—
	8	12.4	58.6	1.08	—	36.8	44.5	2.53	—
	9	16.3	48.3	1.45	—	36.6	38.8	2.64	—
Peri-infarct	7	30.3	44.7	2.03	—	37.3	44.8	2.48	—
Misery perfusion	8	26.9	64.5	2.70	—	33.6	48.5	2.55	—
	9	29.8	48.8	2.67	—	37.7	37.8	2.65	—
Remote area in cerebrum	2	31.1	37.2	1.98	—	51.6	32.4	2.84	—
	3	32.8	49.2	1.95	—	40.8	49.3	2.43	—
	4	nq	—	—	4.56	nq	—	—	6.15
	6	nq	—	—	7.20	nq	—	—	9.46
Remote area in cerebellum	2	34.2	41.5	2.42	—	48.1	35.7	2.93	—
	3	48.3	52.8	3.08	—	51.9	53.2	3.34	—
	4	41.3	39.9	2.80	—	48.1	40.9	3.39	—
	5	nq	—	—	4.28	nq	—	—	4.95
	6	nq	—	—	6.88	nq	—	—	8.37

— = not done; nq = quantification of the absolute rCBF value was not performed.

animal models (*22*) and in a CT-negative area in autopsied human brain (*23*). Sette et al. (*11*) observed not only a decrease in ^{11}C-flumazenil uptake but also an increase in ^{11}C-PK11195 uptake (a ligand for the peripheral type of BZD receptor), suggesting neuronal damage and a glial/macrophagic reaction in the peri-infarct area. Furthermore, the degree of BZD receptor decrease was less severe in the peri-infarct area than in the infarct, which is consistent with the findings of an earlier report (*12*). Mies et al. (*22*) observed a gradual decrease in the number of cortical neurons from the nonaffected area to the peri-infarct zone, although the infarcts were sharply demarcated macroscopically. Cortical neurons in the peri-infarct area are thus thought to suffer less damage compared to the infarcted area. These results suggest that the relatively mild decrease in BZD receptors associated with hypoperfusion and hypometabolism in the peri-infarct area may be due not to deafferentation but rather to neuronal damage.

The peri-infarct areas observed in this study were relatively small and not widely extended. There is a possibility that the CBF, cerebral metabolism and ^{123}I-IMZ uptake in such lesions may be underestimated due to the limited spatial resolution of both the PET and SPECT systems compared with MRI. This may have caused the decreases in the results of both PET and SPECT images in areas with normal MRI findings. Further studies using devices with higher resolution are required to resolve this problem.

Benzodiazepine Receptors in Misery Perfusion

Decreased perfusion associated with an increased OEF has been reported in patients with a transient ischemic attack (*24*). A focal increase in OEF indicates that the oxygen supply is low relative to demand, a situation referred to as "misery perfusion" (*25*). Even if oxygen metabolism is not decreased in the brain, the symptom of transient ischemia could be triggered by a further decrease in the perfusion pressure. In addition, no morphological abnormalities were demonstrated in the misery perfusion area on MRI, as was previously found by CT scan (*26*). Improvement in the clinical symptoms and cerebral perfusion in patients with misery perfusion after bypass surgery (*25,26*), therefore, may indicate neuronal viability in such lesions. In this study, ^{123}I-IMZ uptake was preserved in the misery perfusion area. This suggests that the BZD receptor density may reflect neuronal cell viability in spite of the hypoperfusion.

Benzodiazepine Receptors in Remote Areas

Iodine-123-IMZ uptake was preserved or minimally decreased in the remote areas, including 26 regions in the ipsilateral cerebral cortices and five in the contralateral cerebellum (crossed cerebellar diaschisis). Hatazawa et al. (*12*) also observed hypoperfusion associated with normal ^{123}I-IMZ uptake in such regions. Although hypoperfusion and hypometabolism without any morphological abnormalities are sometimes observed in the cerebral cortex overlying a deep infarct, these findings cannot differentiate between the remote area and the peri-infarct area. Sette et al. (*11*) observed decreased blood flow and decreased oxygen metabolism in the cerebral cortex overlying a deep infarct. They did not observe any changes in either ^{11}C-PK11195 uptake or ^{11}C-flumazenil uptake and thus considered the area as a remote deafferentated area without any neuronal damage. The BZD receptor is thus considered to be able to differentiate remote noninfarcted areas from peri-infarct areas.

In remote areas in the contralateral cerebellum, both the blood flow and the metabolism showed a decrease without any morphological abnormalities (*27,28*). In an animal model using autoradiographic techniques, a low uptake of ^{14}C-2-deoxyglucose and normal binding of ^{123}I-IMZ in the remote areas were also demonstrated (*21*). The BZD receptor distribution is, therefore, considered to provide information that is different from that of either the blood flow or metabolism.

Analytical Problems

We did not perform quantification of the BZD receptor density in this study. Both visual analysis and the L-to-C ratio are considered to be empirical methods because they may not be able to eliminate factors affecting ^{123}I-IMZ uptake, such as the CBF, nonspecific binding, peripheral clearance or binding to plasma proteins (*29–32*). Methods for in vivo quantification of neuroreceptors can be broadly divided into kinetic (*29,30*) and equilibrium methods (*29,31*), measuring either the receptor density (B_{max}) and the affinity (K_D) or the binding potential (BP), which is derived as B_{max}/K_D. Such methods are not thought to be applicable for clinical use because they require prolonged dynamic data acquisition and serial arterial blood sampling. Although the limitations of empirical methods are well understood, the usefulness of ^{123}I-IMZ SPECT for clinical application has been reported using either visual analysis or the count ratio (*9,10,12*). Because nonspecific binding was less than 19% of the cortical radioactivity (*7,29,32*), analysis of ^{123}I-IMZ SPECT by empirical methods may predominantly reflect specific binding. Although there remains a possibility that an alteration of the CBF can change the ^{123}I-IMZ uptake in lesions, in this study, preserved ^{123}I-IMZ uptake was observed in both misery perfusion areas and remote deafferented areas with hypoperfusion. Onishi et al. (*33*) revealed that ^{123}I-IMZ SPECT images that are least affected by the CBF can be obtained about 3–3.5 hr after administration. They also found that the ^{123}I-IMZ SPECT image contrast in five patients at 3 hr postinjection agreed well with the reference receptor binding estimated by kinetic analysis, with a mean error of 3.6%. They showed that ^{123}I-IMZ SPECT images provided the same information as parametric images of the distribution volume in a patient with cerebral infarction. Thus, alteration of the CBF is not considered to change mainly the ^{123}I-IMZ uptake. In addition, empirical methods are simple and noninvasive and thus can be used as an initial form of analysis. Recently, a simple noninvasive method based on the three-compartment, two-parameter model for quantification was reported to be useful for quantification (*32*). This method requires only two separate SPECT scans and a single venous blood sample. Establishment of simple methods for quantification may provide more accurate information from ^{123}I-IMZ SPECT for assessing neuronal damage.

A significant difference between ^{123}I-IMZ uptake and either the CBF or the cerebral metabolism was observed only in the remote areas. Although we could not obtain a definite conclusion due to the limited number of subjects, our results support the findings of earlier studies (*11,12*) and strongly suggest the usefulness of ^{123}I-IMZ SPECT for assessing neuronal damage. The subjects consisted of both patients with cerebral infarction due to either atherosclerosis or arteritis and those with moyamoya disease. Although the etiology of moyamoya disease is unknown and is thought to differ from that of both atherosclerosis and arteritis, the pathological features of lesions in the cerebrum are those of ischemic changes. Because the purpose of this study was to examine the BZD receptor density in ischemic lesions, we included patients with moyamoya disease as subjects of this study. In moyamoya disease, bilateral involvement could be another problem. In two cases with moyamoya disease (Patients 7 and 9), the reference region was not exactly the

contralateral mirror region because multiple ischemic lesions were observed in the bilateral cerebral cortices. Although the reference region was placed in the suspected normal area in the contralateral cerebral artery territory, the possibility of changes in the BZD receptor density in the bilateral cerebral cortices cannot be excluded. In such patients, quantification of the BZD receptor density may provide useful clinical information.

CONCLUSION

The BZD receptor distribution, as measured by ^{123}I-IMZ SPECT, is not considered to reflect the neuronal function. Rather, it may reflect the neuronal cell viability, which is different from both the CBF and the cerebral metabolism. Therefore, ^{123}I-IMZ SPECT is considered to be a potential probe for neuronal damage. Further studies in an increased number of subjects and with quantitative measurement of the BZD receptor density should improve its accuracy.

ACKNOWLEDGMENTS

We thank Drs. Lawrence Buadu and Lawrence W. Stiver for their editorial assistance and the technologists in the Division of Nuclear Medicine at Kyushu University Hospital for their technical assistance. The authors also thank Nihon Medi-Physics Co., Ltd. (Nishinomiya, Japan), for providing ^{123}I-IMZ.

REFERENCES

1. Mazière M, Hantraye P, Prenant C, Sastre J, Comar D. Synthesis of ethyl 8-fluoro-5,6-dihydro-5-[^{11}C]methyl-6-oxo-4H-imidazo[1,5-a][1,4]benzodiazepine-3-carboxylate (RO 15.1788-^{11}C): a specific radioligand for the in vivo study of central benzodiazepine receptors by positron emission tomography. *Int J Appl Radiat Isot* 1984;35:973–976.
2. Samson Y, Hantraye P, Baron JC, Soussaline F, Comar D, Mazière M. Kinetics and displacement of [^{11}C]RO 15-1788, a benzodiazepine antagonist, studied in human brain in vivo by positron tomography. *Eur J Pharmacol* 1985;110:247–251.
3. Persson A, Ehrin E, Eriksson L, et al. Imaging of [^{11}C]-labeled RO 15-1788 binding to benzodiazepine receptors in the human brain by positron emission tomography. *J Psychiatr Res* 1985;19:609–622.
4. Shinotoh H, Yamasaki T, Inoue O, et al. Visualization of specific binding sites of benzodiazepine in human brain. *J Nucl Med* 1986;27:1593–1599.
5. Savic I, Persson A, Roland P, Pauli S, Sedvall G, Widén L. In vivo demonstration of reduced BZ receptor binding in human epileptic foci. *Lancet* 1988;2:863–866.
6. Savic I, Ingvar M, Stone-Elander S. Comparison of [^{11}C]flumazenil and [^{18}F]FDG as PET markers of epileptic foci. *J Neurol Neurosurg Psychiatry* 1993;56:615–621.
7. Beer HF, Bläuenstein PA, Hasler PH, et al. In vitro and in vivo evaluation of iodine-123-RO 16-0154: a new imaging agent for SPECT investigations of benzodiazepine receptors. *J Nucl Med* 1990;31:1007–1014.
8. Ferstl FJ, Cordes M, Cordes I, et al. 123-I-iomazenil-SPECT in patients with focal epilepsies: a comparative study with ^{99m}Tc-HMPAO-SPECT, CT and MR. *Adv Exp Med Biol* 1991;287:405–412.
9. Bartenstein P, Ludolph A, Schober O, et al. Benzodiazepine receptors and cerebral blood flow in partial epilepsy. *Eur J Nucl Med* 1991;18:111–118.
10. Schubiger PA, Hasler PH, Beer-Wohlfahrt H, et al. Evaluation of a multicentre study with iomazenil: a benzodiazepine receptor ligand. *Nucl Med Commun* 1991;12:569–582.
11. Sette G, Baron J-C, Young AR, et al. In vivo mapping of brain benzodiazepine receptor changes by positron emission tomography after focal ischemia in the anesthetized baboon. *Stroke* 1993;24:2046–2058.
12. Hatazawa J, Satoh T, Shimosegawa E, et al. Evaluation of cerebral infarction with iodine-123-iomazenil SPECT. *J Nucl Med* 1995;36:2154–2161.
13. Frackowiack RS, Lenzi GL, Jones T, Heather JD. Quantitative measurement of regional cerebral blood flow and oxygen metabolism in man using ^{15}O and positron emission tomography: theory, procedure and normal value. *J Comput Assist Tomogr* 1980;4:727–736.
14. Kuwabara Y, Ichiya Y, Otsuka M, et al. Cerebral hemodynamic changes in the child and the adult with moyamoya disease. *Stroke* 1990;21:272–277.
15. Lassen NA, Anderson AR, Friberg L, Paulsen OB. The retention of [Tc-99m]-D,L-HM-PAO in the human brain after intracarotid bolus injection: a kinetic analysis. *J Cereb Blood Flow Metab* 1988;8(suppl):s13–s22.
16. Lammertsma AA, Jones T. Correction for the presence of intravascular oxygen-15 in the steady state technique for measuring regional oxygen extraction ratio in the brain: 1. Description of the method. *J Cereb Blood Flow Metab* 1983;3:416–424.
17. Phelps ME, Huang SC, Hoffman EJ, et al. Tomographic measurements of local cerebral glucose metabolic rate in humans with [^{18}F]2-fluoro-2-deoxy-D-glucose: validation of method. *Ann Neurol* 1979;6:371–388.
18. Brooks RA. Alternative formula for glucose utilization using labeled deoxyglucose. *J Nucl Med* 1982;23:538–539.
19. Onodera H, Sato G, Kogure K. GABA and benzodiazepine receptors in the gerbil brain after transient ischemia: demonstration by quantitative receptor autoradiography. *J Cereb Blood Flow Metab* 1987;7:82–88.
20. Matsuda H, Tsuji S, Kuji I, Hisada K. Central type benzodiazepine receptor and cerebral blood flow in experimental chronic brain infarction: evaluation using a double tracer autoradiography technique. *Jpn J Nucl Med* 1993;30:643–650.
21. Odano I, Miyashita K, Minoshima S, et al. A potential use of a ^{123}I-labeled benzodiazepine receptor antagonist as predictor of neuronal cell viability: comparison with ^{14}C-labeled 2-deoxyglucose autoradiography and histopathological examination. *Nucl Med Commun* 1995;16:443–446.
22. Mies G, Auer LM, Ebhardt G, Traupe H, Heiss WD. Flow and neuronal density in tissue surrounding chronic infarction. *Stroke* 1983;14:22–27.
23. Lassen NA, Olsen TS, Hojgaard K, Skriver E. Incomplete infarction: a CT-negative irreversible ischemic brain infarcts. *J Cereb Blood Flow Metab* 1983;3(suppl):S602–S603.
24. Lenzi GL, Jones T, McKenzie CG, Moss S. Non-invasive regional study of chronic cerebrovascular disorders using the oxygen 15 inhalation technique. *J Neurol Neurosurg Psychiatry* 1978;41:11–17.
25. Baron JC, Bousser MG, Rey A, Guillard A, Comar D, Castaigne P. Reversal of focal "misery-perfusion syndrome" by extra-intracranial artery bypass in hemodynamic cerebral ischemia. *Stroke* 1981;12:454–459.
26. Bousser MG, Baron JC, Iba-Zizen MT, Comar D, Cabanis E, Castaigne P. Migrainous cerebral infarction: a tomographic study of cerebral blood flow and oxygen extraction fraction with the oxygen-15 inhalation technique. *Stroke* 1980;11:145–148.
27. Baron JC, Bousser MG, Comar D, Castaigne P. "Crossed cerebellar diaschisis" in human supratentorial brain infarction. *Trans Am Neurol Assoc* 1980;105:459–461.
28. Pantano P, Baron JC, Samson Y, Bousser MG, Derouesne C, Comar D. Crossed cerebellar diaschisis: further studies. *Brain* 1986;109:677–694.
29. Abi-Dargham A, Laruelle M, Seibyl J, et al. SPECT measurement of benzodiazepine receptors in human brain with iodine-123-iomazenil: kinetic and equilibrium paradigms. *J Nucl Med* 1994;35:228–238.
30. Laruelle M, Baldwin RM, Rattner Z, et al. SPECT quantification of [^{123}I]iomazenil binding to benzodiazepine receptors in nonhuman primates: I. Kinetic modeling of single bolus experiments. *J Cereb Blood Flow Metab* 1994;14:439–452.
31. Laruelle M, Abi-Dargham A, Al-Tikriti MS, et al. SPECT quantification of [^{123}I]iomazenil binding to benzodiazepine receptors in nonhuman primates: II. Equilibrium analysis of constant infusion experiments and correlation with *in vitro* parameters. *J Cereb Blood Flow Metab* 1994;14:453–465.
32. Onishi Y, Yonekura Y, Nishizawa S, et al. Noninvasive quantification of iodine-123-iomazenil SPECT. *J Nucl Med* 1996;37:374–378.
33. Onishi Y, Yonekura Y, Tanaka F, et al. Delayed image of iodine-123 iomazenil as a relative map of benzodiazepine receptor binding: the optimal scan time. *Eur J Nucl Med* 1996;23:1491–1497.